

Bottom-heavy initial mass functions reveal hidden mass in early galaxies

Chloe M. Cheng^{1*}, Martje Slob¹, Mariska Kriek¹,
Aliza G. Beverage², Pieter G. van Dokkum³, Rachel Bezanson⁴,
Gabriel Brammer^{5, 6}, Charlie Conroy⁷, Anna de Graaff^{7, 8},
Elham Eftekhari¹, Robert Feldmann⁹, Wout M. Goesaert¹,
Meng Gu^{10, 11}, Joel Leja^{12, 13, 14}, Brian Lorenz¹⁵,
Pavel E. Mancera Piña¹, Ignacio Martín-Navarro^{16, 17},
Andrew B. Newman², Sedona H. Price¹⁸, Alice E. Shapley¹⁹,
Piyush Sharda¹, Katherine A. Suess²⁰, Arjen van der Wel²¹,
Daniel R. Weisz¹⁵

¹*Leiden Observatory, Leiden University, P.O. Box 9513, 2300RA
Leiden, The Netherlands.

²Observatories of the Carnegie Institution for Science, 813 Santa
Barbara Street, Pasadena, CA 91101, USA.

³Astronomy Department, Yale University, 52 Hillhouse Ave, New
Haven, CT 06511, USA.

⁴Department of Physics & Astronomy and PITT PACC, University of
Pittsburgh, Pittsburgh, PA 15260, USA.

⁵Cosmic Dawn Center (DAWN), Denmark.

⁶Niels Bohr Institute, University of Copenhagen, Jagtvej 128, 2200
Copenhagen N, Denmark.

⁷Center for Astrophysics | Harvard & Smithsonian, Cambridge, MA
02138, USA.

⁸Max-Planck-Institut für Astronomie, Königstuhl 17, D-69117
Heidelberg, Germany.

⁹Department of Astrophysics, Universität Zürich, Zurich CH-8057,
Switzerland.

¹⁰Department of Astronomy, Tsinghua University, Beijing 100084,
People's Republic of China.

¹¹Hong Kong Institute for Astronomy & Astrophysics, Pokfulam Road,
The University of Hong Kong.

¹²Department of Astronomy & Astrophysics, The Pennsylvania State University, University Park, PA 16802, USA.

¹³Institute for Computational & Data Sciences, The Pennsylvania State University, University Park, PA 16802, USA.

¹⁴Institute for Gravitation and the Cosmos, The Pennsylvania State University, University Park, PA 16802, USA.

¹⁵Department of Astronomy, University of California, Berkeley, CA 94720, USA.

¹⁶Instituto de Astrofísica de Canarias, c/ Vía Láctea s/n, E38205 - La Laguna, Tenerife, Spain.

¹⁷Departamento de Astrofísica, Universidad de La Laguna, E-38205 La Laguna, Tenerife, Spain.

¹⁸Space Telescope Science Institute (STScI), 3700 San Martin Drive, Baltimore, MD 21218, USA.

¹⁹Department of Physics & Astronomy, University of California, Los Angeles, 430 Portola Plaza, Los Angeles, CA 90095, USA.

²⁰Department for Astrophysical & Planetary Science, University of Colorado, Boulder, CO 80309, USA.

²¹Sterrenkundig Observatorium, Universiteit Ghent, Krijgslaan 281 S9, B-9000 Gent, Belgium.

*Corresponding author(s). E-mail(s): cheng@strw.leidenuniv.nl;

Abstract

JWST observations have revealed that massive galaxies formed and evolved far faster than predicted by galaxy formation models, with many having already assembled a large mass in stars ~ 12 billion years ago [1–7]. However, masses of distant galaxies are highly uncertain, as they assume a distribution of stellar birth masses (the initial mass function [IMF]) similar to that in the Milky Way (MW). Specifically, the contribution from low-mass stars, which make up the bulk of stellar mass, is not directly observed, but inferred based on an extrapolation of the MW IMF. Here, we provide the first robust measurements of the IMF beyond the local Universe. Using ultra-deep spectra of nine massive, quiescent galaxies at $z \sim 0.7$ from the ambitious *JWST*-IMFERN0 program, extended to bluer wavelengths with deep spectra from LEGA-C [8], we find that these distant galaxies have excess low-mass stars. In other words, they have more bottom-heavy IMFs than the MW. For the oldest two galaxies, which are direct descendants of *JWST*'s “impossibly early” galaxies, the bottom-heavy IMFs increase their stellar masses by a factor of **3 – 4**. These galaxies thus amplify the tension with galaxy formation models.

Keywords: galaxies: abundances, galaxies: evolution, galaxies: formation, galaxies: stellar content

We examine nine massive, quiescent galaxies at $z \sim 0.7$, observed via the *JWST*-IMFERO program. Targets were selected from the LEGA-C survey [8], on the basis of their quiescent stellar populations, redshifts, H -band magnitudes, and availability of COSMOS-Web photometry ([5, 9, 10], see Methods). The IMFERO spectra were obtained with the *JWST*-NIRSpec/MSA, using the G140M-F100LP disperser-filter combination. Combined with the bluer LEGA-C spectra, the average rest-frame wavelength coverage is $\sim 3700 - 10780$ Å. To robustly constrain the IMF, we require a median S/N $\gtrsim 15$ Å $^{-1}$ for the LEGA-C spectra and a median S/N $\gtrsim 80$ Å $^{-1}$ for the IMFERO spectra, which we determine via mock spectra tests similar to [11]. On the LEGA-C side, the high rest-optical S/N allows us to constrain ages and elemental abundance patterns required to break strong degeneracies between abundance and IMF variations [12–14]. On the IMFERO side, we require higher rest-near-infrared S/N as we target much fainter spectral features, sensitive to the relative fraction of red dwarfs to red giants. We show the nine IMFERO spectra in Figure 1, and the corresponding LEGA-C spectra in Extended Data Figure 6. We show an example combined LEGA-C + IMFERO spectrum in Extended Data Figure 5. Our sample properties are reported in Extended Data Table 1.

To constrain the IMF, we simultaneously fit the entire rest-frame wavelength range covered by LEGA-C and IMFERO with the ABSORPTION LINE FITTER (ALF), a flexible full-spectrum stellar population synthesis (SPS) code [12, 15]. ALF is unique amongst SPS codes in that it can account for variability in abundance patterns and the low-mass shape of the IMF. This flexibility, along with our broad wavelength range, allows us to disentangle degeneracies between elemental abundance and IMF variations [12–14]. We adopt a single-age stellar population, where age, 18 elemental abundances, and the two low-mass slopes of a double broken power-law IMF can vary freely (see Methods and Extended Data Figure 4). To enable comparison with previous work, we also fit the spectra with a Kroupa IMF [16], referred to as the Milky Way (MW) IMF going forward. We additionally test adopting a two-component star-formation history (SFH) comprised of two bursts of star formation with free ages and a parameter representing the relative mass fraction of the young component. The results from this more complex SFH are consistent within uncertainties with those of the single-age model. Thus, we present only the single-age model.

We show the fits to the IMFERO spectra in Figure 1, along with galaxy RGB images from COSMOS-Web [5, 9, 10]. We show the LEGA-C fits in Extended Data Figure 6, although note that we fit the LEGA-C and IMFERO spectra for each galaxy simultaneously. We also show an example full spectrum and best-fitting model in Extended Data Figure 5.

Our ALF fit results are summarized in Figure 2 and reported in Table 2. We show the IMF mismatch parameter (α_{IMF}), which is the ratio between the mass-to-light (M/L) ratio where we allow the IMF to vary freely and the M/L ratio where we fix a MW IMF. As the luminosity is the same for each IMF characterisation, α_{IMF} represents the stellar mass excess compared to the MW. We derive M/L ratios in the rest-frame *HST*/ACS-F814W band. The dashed line represents where galaxies with a MW IMF would lie, with anything above this line considered to be bottom-heavy. We colour-code each point by virial mass ($\log(M_{\text{vir}}/M_{\odot})$, see [23] and Methods). We

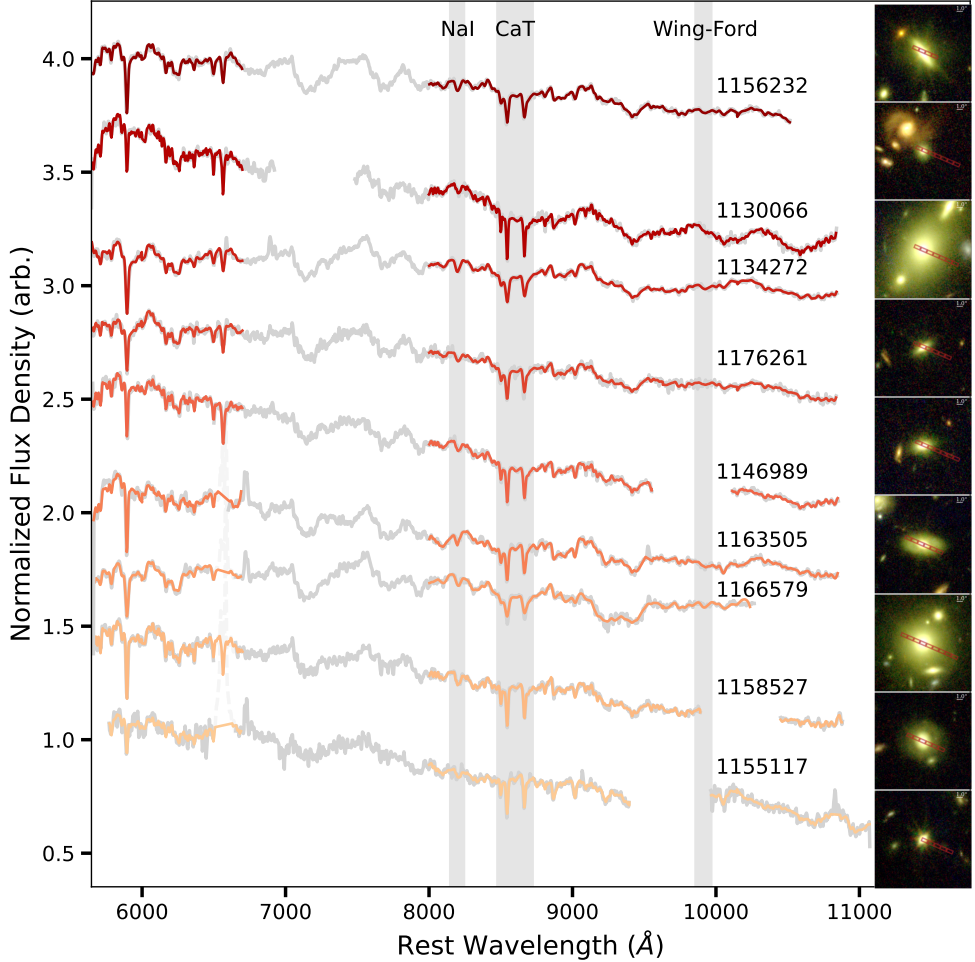


Fig. 1 *JWST*-NIRSpec/MSA spectra (grey) and best-fit stellar population models (coloured lines) for our sample of 9 massive, quiescent galaxies at $z \sim 0.7$, observed via the IMFERN program. Spectra are shown in order of increasing redshift (bottom to top). We normalize each spectrum by the median flux between rest-frame 7500 – 7600 Å, arbitrarily offsetting them in the y -direction for visibility. We indicate key IMF-sensitive absorption features with shaded regions. We do not fit the region between 7000 – 8000 Å due to broad TiO absorption (see Methods). We also show the RGB image cutout (8.5 arcsec \times 8.5 arcsec) for each galaxy next to its corresponding spectrum, where we have combined the F115W, F277W, and F444W COSMOS-Web images [5, 9, 10].

compare α_{IMF} 's to integrated stellar velocity dispersions (σ_v , see Methods) and [Fe/H] ratios (from our ALF fits). For comparison, we show analogous literature measurements from massive, nearby elliptical galaxies (grey, [13, 14, 17, 18]) and lensing/dynamical measurements from massive, nearby ellipticals (blue, [19–21]).

Figure 2 demonstrates that several of our galaxies have α_{IMF} significantly higher than 1, indicating that they have an excess of low-mass stars compared to the MW

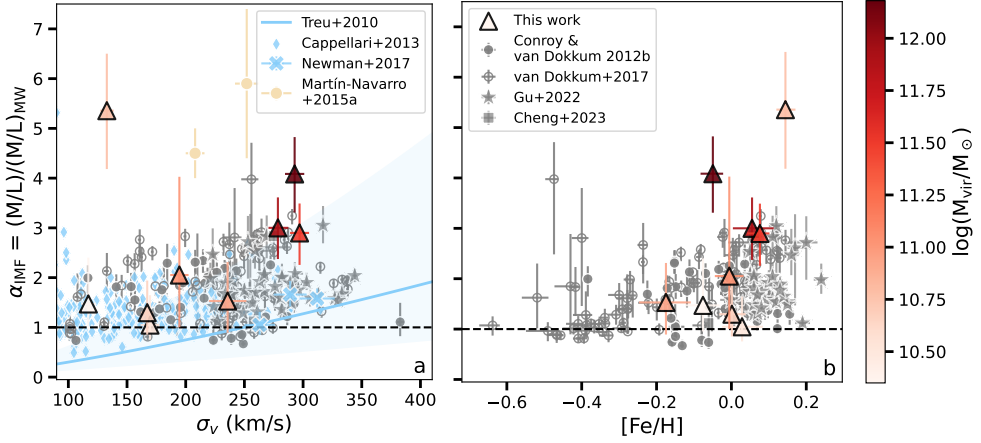


Fig. 2 IMF mismatch parameter (α_{IMF}) – the ratio between the mass-to-light (M/L) ratio where we allow the IMF to vary freely and the M/L ratio where we fix a MW IMF – as a function of stellar velocity dispersion (σ_v ; panel a) and iron abundance ($[\text{Fe}/\text{H}]$; panel b). The IMFFERNO galaxies are shown as triangles, colour-coded by virial masses ($\log(M_{\text{vir}}/M_{\odot})$). Grey symbols represent measurements for massive, elliptical galaxies in the nearby Universe, from [13] (re-derived in [17]), [18], [14], and [17]. Blue symbols represent lensing or dynamical measurements in the nearby Universe, from [19–21]. Beige circles represent spectral index constraints from stacked spectra at $z \sim 1.1$, from [22]. Error bars are 1 standard deviation.

(see Extended Data Figure 4). In other words, their IMFs are bottom-heavy. We primarily find bottom-heavy IMFs in galaxies with higher σ_v , $[\text{Fe}/\text{H}]$, and $\log(M_{\text{vir}}/M_{\odot})$. Qualitatively similar trends were found in the nearby Universe, using similar and complementary methods ([13, 18–20, 24, 25], see also [26]). Thus, we show that these trends were already in place at $z \sim 0.7$, 7 billion years ago. Our results are also consistent with indications from [22], who constrained the IMF in two galaxy stacks at $z \sim 1.1$ using the IMF-sensitive TiO₂ index (beige circles in Figure 2). While our individual-galaxy constraints from full-spectrum fitting are more robust, it is encouraging that distant galaxy stacks exhibit qualitatively similar IMF behaviour.

We note that our most bottom-heavy galaxy, 1158527 ($\alpha_{\text{IMF}} = 5.36^{+1.15}_{-1.17}$, $\sigma_v = 133 \pm 6 \text{ km/s}$), is a clear outlier, as it does not follow the expected trends between α_{IMF} and σ_v and α_{IMF} and $\log(M_{\text{vir}}/M_{\odot})$. However, as this galaxy is quite round (axis ratio of 0.97, see Methods) and is possibly a face-on disc, σ_v (a line-of-sight measurement) may not capture the full gravitational potential. Consequently, $\log(M_{\text{vir}}/M_{\odot})$ may be significantly underestimated. Its high $[\text{Fe}/\text{H}]$ may also point to σ_v being unrepresentative of the galaxy's gravitational potential (see, e.g., [27]).

In our analysis we have only studied the stellar components of our galaxies, and it is important to consider whether our inferred IMFs are realistic when accounting for non-baryonic matter. Thus, as an independent diagnostic, we compare virial (see Methods) and stellar masses in Figure 3. We show stellar masses, estimated using MAGPHYS [28] and assuming a MW IMF [29], as grey circles. We correct the MAGPHYS masses

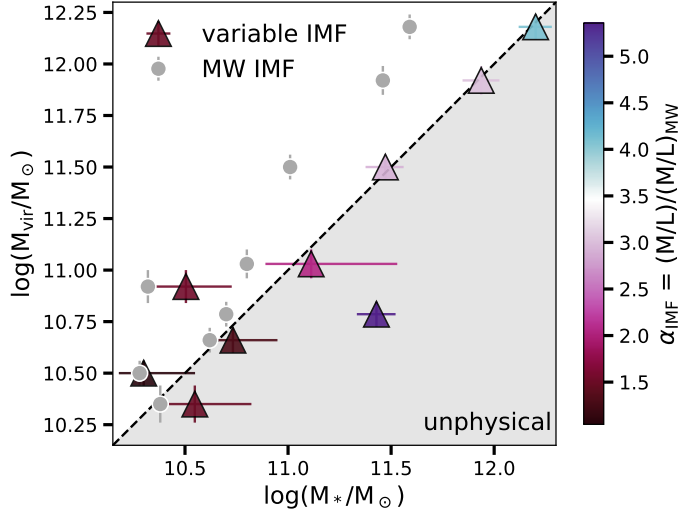


Fig. 3 Comparison between stellar and virial masses. Virial masses ($\log(M_{\text{vir}}/M_{\odot})$) are shown on the y -axis (see Methods). Stellar masses, derived using MAGPHYS ([28, 29]) and assuming a MW IMF, are shown on the x -axis (grey circles). We correct these masses for our best-fit IMF by multiplying them with α_{IMF} . We show the corrected masses as triangles, colour-coded by α_{IMF} . Error bars are 1 standard deviation. The dashed line represents a one-to-one comparison.

for our best-fit IMF by multiplying them by α_{IMF} , and show these corrected masses as triangles colour-coded by α_{IMF} .

Figure 3 shows that, when assuming a MW IMF, the offset between virial and stellar masses increases towards higher mass. Similar results have been found by [30–34]. Interestingly, the stellar masses increase when applying our variable IMF, with the galaxies with the largest mass offsets shifting the most. This stellar mass increase generally brings the stellar and virial masses into agreement. In particular, the stellar masses do *not* exceed the virial masses within uncertainties, reinforcing the physical feasibility of bottom-heavy IMFs in these galaxies (see also [35]). Galaxy 1158527 is the only outlier (similar to Figure 2), falling into unphysical territory. However, as discussed above, we suspect that its virial mass is underestimated due to its face-on inclination. Alternatively, its $[\text{Fe}/\text{H}]$ and/or α_{IMF} constraints could be incorrect, although there are no indications of this from our ALF fits.

The excellent consistency between the virial and IMF-corrected stellar masses in Figure 3 leaves little room for dark matter and gas. However, this is not unexpected as these galaxies have small effective radii (median ~ 5.4 kpc) and thus the virial masses primarily capture their star-dominated central regions (see, e.g. [36]). Additionally, little interstellar gas is expected to be present in massive, quiescent galaxies at these redshifts (e.g., [37]). Moreover, the virial masses may be underestimated as we do not correct σ_v for slit-loss effects, which are complex with the NIRSpec/MSA [34]. In addition, these galaxies may be rotating [38, 39], in which case their σ_v 's would be a poor tracer of their potential wells, contributing to the possible underestimation of the virial masses. This underestimation would allow for more non-baryonic matter.

Detailed dynamical modeling is required to fully account for these effects ([34], Slob et al. in prep.).

Our finding of bottom-heavy IMFs at early times is consistent with the two-phase formation model for massive galaxies, in which the cores of massive, quiescent galaxies are in place at early times (with their central densities staying constant), with their outskirts subsequently building up via minor mergers [40–45]. Specifically, the cores of present-day, massive, early-type galaxies – the likely descendants of our distant systems – have also been found to have bottom-heavy IMFs (e.g., [13, 14, 18]). Moreover, a few of our galaxies may be even more bottom-heavy than nearby galaxy cores. Thus, in the two-phase scenario, the mixing of stellar populations by merging activity may reduce the bottom-heavy nature of the IMF over time in such galaxies.

We examine the four galaxies for which we find the most bottom-heavy IMFs (i.e. inconsistent with a MW IMF by $> 2\sigma$) in detail. Two of them (galaxy IDs 1134272 and 1166579) have the oldest ages and earliest formation times of our sample, implying formation redshifts of $z_{\text{form}} > 6$. Although we expect older galaxies to have slightly higher α_{IMF} 's (as more of their high-mass stars have died), this effect would be $< 10\%$ for the ages covered by our sample and thus cannot explain the high α_{IMF} 's. Assuming a typical star formation timescale of $\sim 100 - 200$ million years [46, 47], these two oldest galaxies were quiescent by $z \sim 5.5$ and are likely the descendants of the “impossibly early” galaxies discovered with *JWST* [2–7]. The formation redshifts of these two oldest and most bottom-heavy galaxies imply that *JWST*'s distant, massive galaxies also had bottom-heavy IMFs at early times, possibly making them a factor of 3 – 4 *more massive* than originally reported. These larger masses would suggest an even greater tension with galaxy formation models ([1–7]).

In this work, we have presented novel measurements of the IMF in the early Universe, using state-of-the-art *JWST* data and sophisticated modelling methods. However, some limitations should be considered when interpreting our results. First, though our spectra have an unprecedented depth at these redshifts, the error bars on our measurements are still large. By extending our spectra to longer wavelengths and examining redder IMF-sensitive spectral features, the IMF can be more precisely constrained. However, this also requires further development of stellar population models, as they are not currently able to fully reproduce such spectra of nearby galaxies [48, 49].

Another limitation of our analysis is that we fix the slope of the IMF beyond $1 M_{\odot}$, as our method is only sensitive to the relative fraction of low-to-high-mass stars (see [12]). However, if this slope is shallower than in the MW, the stellar masses at high redshifts can be reduced. We emphasize that our finding of bottom-heavy IMFs does not negate the possibility of our galaxies also having a shallower IMF slope beyond $1 M_{\odot}$. For example, [50] have suggested a concordance IMF with this behaviour, which brings high-redshift observations into better agreement with current galaxy formation models while also reproducing the excess of low-mass stars found in nearby galaxy cores.

In summary, this work represents a major leap forward in understanding massive galaxy assembly. For the first time, we robustly measured the IMF in a sample of massive, quiescent galaxies beyond the nearby Universe. Our finding of bottom-heavy IMFs at $z \sim 0.7$, particularly in our oldest galaxies, implies that the most massive quiescent

galaxies discovered at high redshifts (stellar mass $\gtrsim 10^{11} M_{\odot}$, [1–4, 6, 7]) likely have even higher masses than originally reported. Our results additionally imply that the masses of their star-forming progenitors may also be underestimated, further heightening the tension. Looking forward, IMF measurements at higher redshifts, even closer to the epoch when these “impossibly early” galaxies formed, will clarify this apparent tension with galaxy formation models. Future extremely deep *JWST*/NIRSpec observations are required to make these constraints possible.

Acknowledgements. This work is based on observations made with the NASA/ESA/CSA *JWST*. The data were obtained from the Mikulski Archive for Space Telescopes (MAST) at the Space Telescope Science Institute (STScI), which is operated by the Association of Universities for Research in Astronomy, Inc., under NASA contract NAS 5-03127 for *JWST*. These observations are associated with program *JWST*-GO-5629. Support for program *JWST*-GO-5629 was provided by NASA through a grant from the STScI. This work used the Dutch national e-infrastructure with the support of the SURF Cooperative using grant no. EINF-10017 which is financed by the Dutch Research Council (NWO). Some of the data products presented herein were retrieved from the Dawn *JWST* Archive (DJA). DJA is an initiative of the Cosmic Dawn Center (DAWN), which is funded by the Danish National Research Foundation under grant DNRF140. MK acknowledges funding from the NWO through the award of the Vici grant VI.C.222.047 (project 2010007169). AdG acknowledges support from a Clay Fellowship awarded by the Smithsonian Astrophysical Observatory. PEMP acknowledges the support from the NWO through the Veni grant VI.Veni.222.364. PS is supported by the Leiden University Oort Fellowship and the IAU Gruber Foundation Fellowship.

Author Contributions. MK, AGB, and CMC wrote the primary *JWST* proposal. MS, CMC, MK, and AGB designed the *JWST* observing plan. MS reduced the data and wrote the data reduction text. CMC fit the spectra with ALF, performed the velocity dispersion correction, wrote the remaining text, and created the figures. CMC, MK, and PGvD led the interpretation. All authors contributed to the analysis and interpretation.

Author Information. The authors declare no competing interests. Correspondence and requests for materials should be addressed to CMC. Reprints and permissions information is available at www.nature.com/reprints.

Data Availability. This work makes use of data from the LEGA-C survey. The reduced data can be obtained from the ESO Science Archive Facility (http://archive.eso.org/eso/eso_archive_main.html). The reduced spectra and catalogue have been released by ESO (<http://archive.eso.org/cms/eso-archive-news/Third-and-final-release-of-the-Large-Early-Galaxy-Census-LEGA-C-Spectroscopic-Public-Survey-published.html>) and are also available here: <https://users.ugent.be/~avdrwel/research.html#legac>. For details, see [8].

The *JWST* data analysed in this work were obtained from the Mikulski Archive for Space Telescopes (MAST) at the Space Telescope Science Institute (STScI). The specific observations can be accessed via [10.17909/k0zz-f371](https://doi.org/10.17909/k0zz-f371).

Our sample properties and fit results are published in Extended Data Tables 1 and 2. Other data products generated in the course of this work will be made available upon reasonable request.

Code Availability. The ALF code on which this work is based is publicly available via <https://github.com/cconroy20/alf>. See [12, 15] for details.

References

- [1] Steinhardt, C.L., Capak, P., Masters, D., Speagle, J.S.: The Impossibly Early Galaxy Problem. *ApJ* **824**(1), 21 (2016) <https://doi.org/10.3847/0004-637X/824/1/21> [arXiv:1506.01377](https://arxiv.org/abs/1506.01377) [astro-ph.GA]
- [2] Carnall, A.C., McLeod, D.J., McLure, R.J., Dunlop, J.S., Begley, R., Cullen, F., Donnan, C.T., Hamadouche, M.L., Jewell, S.M., Jones, E.W., Pollock, C.L., Wild, V.: A surprising abundance of massive quiescent galaxies at $3 < z < 5$ in the first data from JWST CEERS. *MNRAS* **520**(3), 3974–3985 (2023) <https://doi.org/10.1093/mnras/stad369> [arXiv:2208.00986](https://arxiv.org/abs/2208.00986) [astro-ph.GA]
- [3] Carnall, A.C., McLure, R.J., Dunlop, J.S., McLeod, D.J., Wild, V., Cullen, F., Magee, D., Begley, R., Cimatti, A., Donnan, C.T., Hamadouche, M.L., Jewell, S.M., Walker, S.: A massive quiescent galaxy at redshift 4.658. *Nature* **619**(7971), 716–719 (2023) <https://doi.org/10.1038/s41586-023-06158-6> [arXiv:2301.11413](https://arxiv.org/abs/2301.11413) [astro-ph.GA]
- [4] Carnall, A.C., Cullen, F., McLure, R.J., McLeod, D.J., Begley, R., Donnan, C.T., Dunlop, J.S., Shapley, A.E., Rowlands, K., Almaini, O., Arellano-Córdova, K.Z., Barrufet, L., Cimatti, A., Ellis, R.S., Grogan, N.A., Hamadouche, M.L., Illingworth, G.D., Koekemoer, A.M., Leung, H.-H., Lovell, C.C., Pérez-González, P.G., Santini, P., Stanton, T.M., Wild, V.: The JWST EXCELS survey: too much, too young, too fast? Ultra-massive quiescent galaxies at $3 < z < 5$. *MNRAS* **534**(1), 325–348 (2024) <https://doi.org/10.1093/mnras/stae2092> [arXiv:2405.02242](https://arxiv.org/abs/2405.02242) [astro-ph.GA]
- [5] Valentino, F., Brammer, G., Gould, K.M.L., Kokorev, V., Fujimoto, S., Jespersen, C.K., Vijayan, A.P., Weaver, J.R., Ito, K., Tanaka, M., Ilbert, O., Magdis, G.E., Whitaker, K.E., Faisst, A.L., Gallazzi, A., Gillman, S., Giménez-Arteaga, C., Gómez-Guijarro, C., Kubo, M., Heintz, K.E., Hirschmann, M., Oesch, P., Onodera, M., Rizzo, F., Lee, M., Strait, V., Toft, S.: An Atlas of Color-selected Quiescent Galaxies at $z > 3$ in Public JWST Fields. *ApJ* **947**(1), 20 (2023) <https://doi.org/10.3847/1538-4357/acbefa> [arXiv:2302.10936](https://arxiv.org/abs/2302.10936) [astro-ph.GA]
- [6] de Graaff, A., Setton, D.J., Brammer, G., Cutler, S., Suess, K.A., Labb  , I., Leja, J., Weibel, A., Maseda, M.V., Whitaker, K.E., Bezanson, R., Boogaard, L.A., Cleri, N.J., De Lucia, G., Franx, M., Greene, J.E., Hirschmann, M., Matthee, J., McConachie, I., Naidu, R.P., Oesch, P.A., Price, S.H., Rix, H.-W., Valentino, F., Wang, B., Williams, C.C.: Efficient formation of a massive quiescent galaxy

at redshift 4.9. *Nature Astronomy* **9**, 280–292 (2025) <https://doi.org/10.1038/s41550-024-02424-3> arXiv:2404.05683 [astro-ph.GA]

[7] Ito, K., Valentino, F., Brammer, G., Hamadouche, M.L., Whitaker, K.E., Kokorev, V., Zhu, P., Kakimoto, T., Wu, P.-F., Antwi-Danso, J., Baker, W.M., Ceverino, D., Faisst, A.L., Farcy, M., Fujimoto, S., Gallazzi, A., Gillman, S., Got-tumukkala, R., Heintz, K.E., Hirschmann, M., Jespersen, C.K., Kubo, M., Lee, M., Magdis, G., Onodera, M., Shimakawa, R., Tanaka, M., Toft, S., Weaver, J.R.: DeepDive: A deep dive into the physics of the first massive quiescent galaxies in the Universe. arXiv e-prints, 2506–22642 (2025) <https://doi.org/10.48550/arXiv.2506.22642> arXiv:2506.22642 [astro-ph.GA]

[8] Wel, A., Bezanson, R., D’Eugenio, F., Straatman, C., Franx, M., Houdt, J., Maseda, M.V., Gallazzi, A., Wu, P.-F., Pacifici, C., Barisic, I., Brammer, G.B., Munoz-Mateos, J.C., Vervalcke, S., Zibetti, S., Sobral, D., Graaff, A., Calhau, J., Kaushal, Y., Muzzin, A., Bell, E.F., Dokkum, P.G.: The large early galaxy astrophysics census (lega-c) data release 3: 3000 high-quality spectra of k_s -selected galaxies at $z > 0.6$. *The Astrophysical Journal Supplement Series* **256**(2), 44 (2021) <https://doi.org/10.3847/1538-4365/ac1356>

[9] Casey, C.M., Kartaltepe, J.S., Drakos, N.E., Franco, M., Harish, S., Paquereau, L., Ilbert, O., Rose, C., Cox, I.G., Nightingale, J.W., Robertson, B.E., Silverman, J.D., Koekemoer, A.M., Massey, R., McCracken, H.J., Rhodes, J., Akins, H.B., Allen, N., Amvrosiadis, A., Arango-Toro, R.C., Bagley, M.B., Bongiorno, A., Capak, P.L., Champagne, J.B., Chartab, N., Chávez Ortiz, Ó.A., Chworowsky, K., Cooke, K.C., Cooper, O.R., Darvish, B., Ding, X., Faisst, A.L., Finkelstein, S.L., Fujimoto, S., Gentile, F., Gillman, S., Gould, K.M.L., Gozaliasl, G., Hay-ward, C.C., He, Q., Hemmati, S., Hirschmann, M., Jahnke, K., Jin, S., Khostovan, A.A., Kokorev, V., Lambrides, E., Laigle, C., Larson, R.L., Leung, G.C.K., Liu, D., Liaudat, T., Long, A.S., Magdis, G., Mahler, G., Mainieri, V., Manning, S.M., Maraston, C., Martin, C.L., McCleary, J.E., McKinney, J., McPartland, C.J.R., Mobasher, B., Pattnaik, R., Renzini, A., Rich, R.M., Sanders, D.B., Sattari, Z., Scognamiglio, D., Scoville, N., Sheth, K., Shuntov, M., Sparre, M., Suzuki, T.L., Talia, M., Toft, S., Trakhtenbrot, B., Urry, C.M., Valentino, F., Vanderhoof, B.N., Vardoulaki, E., Weaver, J.R., Whitaker, K.E., Wilkins, S.M., Yang, L., Zavala, J.A.: COSMOS-Web: An Overview of the JWST Cosmic Origins Survey. *ApJ* **954**(1), 31 (2023) <https://doi.org/10.3847/1538-4357/acc2bc> arXiv:2211.07865 [astro-ph.GA]

[10] Brammer, G.: Grizli. <https://doi.org/10.5281/zenodo.8370018> . <https://doi.org/10.5281/zenodo.8370018>

[11] Cheng, C.M., Kriek, M., Beverage, A.G., van der Wel, A., Bezanson, R., D’Eugenio, F., Franx, M., Mancera Piña, P.E., Nersesian, A., Slob, M., Suess, K.A., van Dokkum, P.G., Wu, P.-F., Gallazzi, A., Zibetti, S.: Age and metal gradients in massive quiescent galaxies at $0.6 \lesssim z \lesssim 1.0$: implications for quenching

and assembly histories. *MNRAS* **532**(3), 3604–3623 (2024) <https://doi.org/10.1093/mnras/stae1739> arXiv:2407.10974 [astro-ph.GA]

[12] Conroy, C., van Dokkum, P.: Counting Low-mass Stars in Integrated Light. *ApJ* **747**(1), 69 (2012) <https://doi.org/10.1088/0004-637X/747/1/69> arXiv:1109.0007 [astro-ph.CO]

[13] Conroy, C., van Dokkum, P.G.: The Stellar Initial Mass Function in Early-type Galaxies From Absorption Line Spectroscopy. II. Results. *ApJ* **760**(1), 71 (2012) <https://doi.org/10.1088/0004-637X/760/1/71> arXiv:1205.6473 [astro-ph.CO]

[14] Gu, M., Greene, J.E., Newman, A.B., Kreisch, C., Quenneville, M.E., Ma, C.-P., Blakeslee, J.P.: The MASSIVE Survey. XVI. The Stellar Initial Mass Function in the Center of MASSIVE Early-type Galaxies. *ApJ* **932**(2), 103 (2022) <https://doi.org/10.3847/1538-4357/ac69ea> arXiv:2110.11985 [astro-ph.GA]

[15] Conroy, C., Villaume, A., van Dokkum, P.G., Lind, K.: Metal-rich, Metal-poor: Updated Stellar Population Models for Old Stellar Systems. *ApJ* **854**(2), 139 (2018) <https://doi.org/10.3847/1538-4357/aaab49> arXiv:1801.10185 [astro-ph.GA]

[16] Kroupa, P.: On the variation of the initial mass function. *MNRAS* **322**(2), 231–246 (2001) <https://doi.org/10.1046/j.1365-8711.2001.04022.x> arXiv:astro-ph/0009005 [astro-ph]

[17] Cheng, C.M., Villaume, A., Balogh, M.L., Brodie, J.P., Martín-Navarro, I., Romanowsky, A.J., van Dokkum, P.G.: Initial mass function variability from the integrated light of diverse stellar systems. *MNRAS* **526**(3), 4004–4023 (2023) <https://doi.org/10.1093/mnras/stad2967> arXiv:2309.14415 [astro-ph.GA]

[18] van Dokkum, P., Conroy, C., Villaume, A., Brodie, J., Romanowsky, A.J.: The Stellar Initial Mass Function in Early-type Galaxies from Absorption Line Spectroscopy. III. Radial Gradients. *ApJ* **841**(2), 68 (2017) <https://doi.org/10.3847/1538-4357/aa7135> arXiv:1611.09859 [astro-ph.GA]

[19] Treu, T., Auger, M.W., Koopmans, L.V.E., Gavazzi, R., Marshall, P.J., Bolton, A.S.: The Initial Mass Function of Early-Type Galaxies. *ApJ* **709**(2), 1195–1202 (2010) <https://doi.org/10.1088/0004-637X/709/2/1195> arXiv:0911.3392 [astro-ph.CO]

[20] Cappellari, M., McDermid, R.M., Alatalo, K., Blitz, L., Bois, M., Bournaud, F., Bureau, M., Crocker, A.F., Davies, R.L., Davis, T.A., de Zeeuw, P.T., Duc, P.-A., Emsellem, E., Khochfar, S., Krajnović, D., Kuntschner, H., Morganti, R., Naab, T., Oosterloo, T., Sarzi, M., Scott, N., Serra, P., Weijmans, A.-M., Young, L.M.: The ATLAS^{3D} project - XX. Mass-size and mass- σ distributions of early-type galaxies: bulge fraction drives kinematics, mass-to-light ratio, molecular gas fraction and stellar initial mass function. *MNRAS* **432**(3), 1862–1893 (2013)

<https://doi.org/10.1093/mnras/stt644> arXiv:1208.3523 [astro-ph.CO]

- [21] Newman, A.B., Smith, R.J., Conroy, C., Villaume, A., van Dokkum, P.: The Initial Mass Function in the Nearest Strong Lenses from SNELLS: Assessing the Consistency of Lensing, Dynamical, and Spectroscopic Constraints. *ApJ* **845**(2), 157 (2017) <https://doi.org/10.3847/1538-4357/aa816d> arXiv:1612.00065 [astro-ph.GA]
- [22] Martín-Navarro, I., Pérez-González, P.G., Trujillo, I., Esquej, P., Vazdekis, A., Domínguez Sánchez, H., Barro, G., Bruzual, G., Charlot, S., Cava, A., Ferreras, I., Espino, N., La Barbera, F., Koekemoer, A.M., Cenarro, A.J.: The Stellar Initial Mass Function at $0.9 < z < 1.5$. *ApJL* **798**(1), 4 (2015) <https://doi.org/10.1088/2041-8205/798/1/L4> arXiv:1407.4455 [astro-ph.GA]
- [23] van der Wel, A., van Hout, J., Bezanson, R., Franx, M., D'Eugenio, F., Straatman, C., Bell, E.F., Muzzin, A., Sobral, D., Maseda, M.V., de Graaff, A., Holden, B.P.: The Mass Scale of High-redshift Galaxies: Virial Mass Estimates Calibrated with Stellar Dynamical Models from LEGA-C. *ApJ* **936**(1), 9 (2022) <https://doi.org/10.3847/1538-4357/ac83c5> arXiv:2208.12605 [astro-ph.GA]
- [24] La Barbera, F., Ferreras, I., Vazdekis, A., de la Rosa, I.G., de Carvalho, R.R., Trevisan, M., Falcón-Barroso, J., Ricciardelli, E.: SPIDER VIII - constraints on the stellar initial mass function of early-type galaxies from a variety of spectral features. *MNRAS* **433**(4), 3017–3047 (2013) <https://doi.org/10.1093/mnras/stt943> arXiv:1305.2273 [astro-ph.CO]
- [25] McDermid, R.M., Cappellari, M., Alatalo, K., Bayet, E., Blitz, L., Bois, M., Bournaud, F., Bureau, M., Crocker, A.F., Davies, R.L., Davis, T.A., de Zeeuw, P.T., Duc, P.-A., Emsellem, E., Khochfar, S., Krajnović, D., Kuntschner, H., Morganti, R., Naab, T., Oosterloo, T., Sarzi, M., Scott, N., Serra, P., Weijmans, A.-M., Young, L.M.: Connection between Dynamically Derived Initial Mass Function Normalization and Stellar Population Parameters. *ApJL* **792**(2), 37 (2014) <https://doi.org/10.1088/2041-8205/792/2/L37> arXiv:1408.3189 [astro-ph.GA]
- [26] Smith, R.J.: Evidence for Initial Mass Function Variation in Massive Early-Type Galaxies. *ARAA* **58**, 577–615 (2020) <https://doi.org/10.1146/annurev-astro-032620-020217>
- [27] Beverage, A.G., Kriek, M., Conroy, C., Sandford, N.R., Bezanson, R., Franx, M., van der Wel, A., Weisz, D.R.: From Carbon to Cobalt: Chemical Compositions and Ages of $z > 0.7$ Quiescent Galaxies. *ApJ* **948**(2), 140 (2023) <https://doi.org/10.3847/1538-4357/acc176> arXiv:2303.03412 [astro-ph.GA]
- [28] da Cunha, E., Charlot, S., Elbaz, D.: A simple model to interpret the ultraviolet, optical and infrared emission from galaxies. *MNRAS* **388**(4), 1595–1617 (2008) <https://doi.org/10.1111/j.1365-2966.2008.13535.x> arXiv:0806.1020 [astro-ph]

[29] de Graaff, A., Bezanson, R., Franx, M., van der Wel, A., Holden, B., van de Sande, J., Bell, E.F., D'Eugenio, F., Maseda, M.V., Muzzin, A., Sobral, D., Straatman, C.M.S., Wu, P.-F.: The Fundamental Plane in the LEGA-C Survey: Unraveling the M/L Ratio Variations of Massive Star-forming and Quiescent Galaxies at $z \sim 0.8$. *ApJ* **913**(2), 103 (2021) <https://doi.org/10.3847/1538-4357/abf1e7> [arXiv:2103.12753](https://arxiv.org/abs/2103.12753) [astro-ph.GA]

[30] van de Sande, J., Kriek, M., Franx, M., van Dokkum, P.G., Bezanson, R., Bouwens, R.J., Quadri, R.F., Rix, H.-W., Skelton, R.E.: Stellar Kinematics of $z \sim 2$ Galaxies and the Inside-out Growth of Quiescent Galaxies. *ApJ* **771**(2), 85 (2013) <https://doi.org/10.1088/0004-637X/771/2/85> [arXiv:1211.3424](https://arxiv.org/abs/1211.3424) [astro-ph.CO]

[31] Belli, S., Newman, A.B., Ellis, R.S.: MOSFIRE Spectroscopy of Quiescent Galaxies at $1.5 < z < 2.5$. I. Evolution of Structural and Dynamical Properties. *ApJ* **834**(1), 18 (2017) <https://doi.org/10.3847/1538-4357/834/1/18> [arXiv:1608.00608](https://arxiv.org/abs/1608.00608) [astro-ph.GA]

[32] Mendel, J.T., Beifiori, A., Saglia, R.P., Bender, R., Brammer, G.B., Chan, J., Förster Schreiber, N.M., Fossati, M., Galametz, A., Momcheva, I.G., Nelson, E.J., Wilman, D.J., Wuyts, S.: The Kinematics of Massive Quiescent Galaxies at $1.4 < z < 2.1$: Dark Matter Fractions, IMF Variation, and the Relation to Local Early-type Galaxies. *ApJ* **899**(1), 87 (2020) <https://doi.org/10.3847/1538-4357/ab9ffcc> [arXiv:2006.13949](https://arxiv.org/abs/2006.13949) [astro-ph.GA]

[33] Kriek, M., Beverage, A.G., Price, S.H., Suess, K.A., Barro, G., Bezanson, R.S., Conroy, C., Cutler, S.E., Franx, M., Lin, J., Lorenz, B., Ma, Y., Momcheva, I.G., Mowla, L.A., Pasha, I., van Dokkum, P., Whitaker, K.E.: The Heavy Metal Survey: Star Formation Constraints and Dynamical Masses of 21 Massive Quiescent Galaxies at $z = 1.3\text{--}2.3$. *ApJ* **966**(1), 36 (2024) <https://doi.org/10.3847/1538-4357/ad2df9> [arXiv:2311.16232](https://arxiv.org/abs/2311.16232) [astro-ph.GA]

[34] Slob, M., Kriek, M., de Graaff, A., Cheng, C.M., Beverage, A.G., Bezanson, R., Förster Schreiber, N.M., Lorenz, B., Mancera Piña, P.E., Marchesini, D., Muzzin, A., Newman, A.B., Price, S.H., Suess, K.A., van de Sande, J., van Dokkum, P., Weisz, D.R.: Fast rotators at cosmic noon: Stellar kinematics for 15 quiescent galaxies from JWST-SUSPENSE. *AA* **702**, 110 (2025) <https://doi.org/10.1051/0004-6361/202555812> [arXiv:2506.04310](https://arxiv.org/abs/2506.04310) [astro-ph.GA]

[35] Lyubenova, M., Martín-Navarro, I., van de Ven, G., Falcón-Barroso, J., Galbany, L., Gallazzi, A., García-Benito, R., González Delgado, R., Husemann, B., La Barbera, F., Marino, R.A., Mast, D., Mendez-Abreu, J., Peletier, R.F.P., Sánchez-Blázquez, P., Sánchez, S.F., Trager, S.C., van den Bosch, R.C.E., Vazdekis, A., Walcher, C.J., Zhu, L., Zibetti, S., Ziegler, B., Bland-Hawthorn, J., CALIFA Collaboration: IMF shape constraints from stellar populations and dynamics from CALIFA. *MNRAS* **463**(3), 3220–3225 (2016) <https://doi.org/10.1093/mnras/463.3.3220>

stw2434 arXiv:1606.07448 [astro-ph.GA]

[36] de Graaff, A., Pillepich, A., Rix, H.-W.: An Early Dark Matter-dominated Phase in the Assembly History of Milky Way-mass Galaxies Suggested by the TNG50 Simulation and JWST Observations. *ApJL* **967**(2), 40 (2024) <https://doi.org/10.3847/2041-8213/ad4c65> arXiv:2403.00907 [astro-ph.GA]

[37] Spilker, J., Bezanson, R., Barišić, I., Bell, E., Lagos, C.d.P., Maseda, M., Muzzin, A., Pacifici, C., Sobral, D., Straatman, C., van der Wel, A., van Dokkum, P., Weiner, B., Whitaker, K., Williams, C.C., Wu, P.-F.: Molecular Gas Contents and Scaling Relations for Massive, Passive Galaxies at Intermediate Redshifts from the LEGA-C Survey. *ApJ* **860**(2), 103 (2018) <https://doi.org/10.3847/1538-4357/aac438> arXiv:1805.02667 [astro-ph.GA]

[38] Bezanson, R., van der Wel, A., Straatman, C., Pacifici, C., Wu, P.-F., Barišić, I., Bell, E.F., Conroy, C., D'Eugenio, F., Franx, M., Gallazzi, A., van Houtd, J., Maseda, M.V., Muzzin, A., van de Sande, J., Sobral, D., Spilker, J.: 1D Kinematics from Stars and Ionized Gas at $z \sim 0.8$ from the LEGA-C Spectroscopic Survey of Massive Galaxies. *ApJL* **868**(2), 36 (2018) <https://doi.org/10.3847/2041-8213/aaf16b> arXiv:1811.07900 [astro-ph.GA]

[39] van Houtd, J., van der Wel, A., Bezanson, R., Franx, M., d'Eugenio, F., Barisic, I., Bell, E.F., Gallazzi, A., de Graaff, A., Maseda, M.V., Pacifici, C., van de Sande, J., Sobral, D., Straatman, C., Wu, P.-F.: Stellar Dynamical Models for 797 $z > 0.8$ Galaxies from LEGA-C. *ApJ* **923**(1), 11 (2021) <https://doi.org/10.3847/1538-4357/ac1f29> arXiv:2108.08142 [astro-ph.GA]

[40] Bezanson, R., van Dokkum, P.G., Tal, T., Marchesini, D., Kriek, M., Franx, M., Coppi, P.: The Relation Between Compact, Quiescent High-redshift Galaxies and Massive Nearby Elliptical Galaxies: Evidence for Hierarchical, Inside-Out Growth. *ApJ* **697**(2), 1290–1298 (2009) <https://doi.org/10.1088/0004-637X/697/2/1290> arXiv:0903.2044 [astro-ph.CO]

[41] Naab, T., Johansson, P.H., Ostriker, J.P.: Minor Mergers and the Size Evolution of Elliptical Galaxies. *ApJL* **699**(2), 178–182 (2009) <https://doi.org/10.1088/0004-637X/699/2/L178> arXiv:0903.1636 [astro-ph.CO]

[42] Feldmann, R., Carollo, C.M., Mayer, L., Renzini, A., Lake, G., Quinn, T., Stinson, G.S., Yepes, G.: The Evolution of Central Group Galaxies in Hydrodynamical Simulations. *ApJ* **709**(1), 218–240 (2010) <https://doi.org/10.1088/0004-637X/709/1/218> arXiv:0906.3022 [astro-ph.CO]

[43] Oser, L., Ostriker, J.P., Naab, T., Johansson, P.H., Burkert, A.: The Two Phases of Galaxy Formation. *ApJ* **725**(2), 2312–2323 (2010) <https://doi.org/10.1088/0004-637X/725/2/2312> arXiv:1010.1381 [astro-ph.CO]

[44] Rodriguez-Gomez, V., Pillepich, A., Sales, L.V., Genel, S., Vogelsberger, M., Zhu,

Q., Wellons, S., Nelson, D., Torrey, P., Springel, V., Ma, C.-P., Hernquist, L.: The stellar mass assembly of galaxies in the Illustris simulation: growth by mergers and the spatial distribution of accreted stars. *MNRAS* **458**(3), 2371–2390 (2016) <https://doi.org/10.1093/mnras/stw456> arXiv:1511.08804 [astro-ph.GA]

[45] Suess, K.A., Kriek, M., Price, S.H., Barro, G.: Color Gradients along the Quiescent Galaxy Sequence: Clues to Quenching and Structural Growth. *ApJL* **899**(2), 26 (2020) <https://doi.org/10.3847/2041-8213/abacc9> arXiv:2008.02817 [astro-ph.GA]

[46] Kriek, M., Conroy, C., van Dokkum, P.G., Shapley, A.E., Choi, J., Reddy, N.A., Siana, B., van de Voort, F., Coil, A.L., Mobasher, B.: A massive, quiescent, population II galaxy at a redshift of 2.1. *Nature* **540**(7632), 248–251 (2016) <https://doi.org/10.1038/nature20570> arXiv:1612.02001 [astro-ph.GA]

[47] Beverage, A.G., Slob, M., Kriek, M., Conroy, C., Barro, G., Bezanson, R., Brammer, G., Cheng, C.M., de Graaff, A., Förster Schreiber, N.M., Franx, M., Lorenz, B., Mancera Piña, P.E., Marchesini, D., Muzzin, A., Newman, A.B., Price, S.H., Shapley, A.E., Stefanon, M., Suess, K.A., van Dokkum, P., Weinberg, D., Weisz, D.R.: Carbon and Iron Deficiencies in Quiescent Galaxies at $z = 1$ –3 from JWST-SUSPENSE: Implications for the Formation Histories of Massive Galaxies. *ApJ* **979**(2), 249 (2025) <https://doi.org/10.3847/1538-4357/ad96b6> arXiv:2407.02556 [astro-ph.GA]

[48] Eftekhari, E., Vazdekis, A., La Barbera, F.: Fingerprints of stellar populations in the near-infrared: an optimized set of spectral indices in the JHK bands. *MNRAS* **504**(2), 2190–2223 (2021) <https://doi.org/10.1093/mnras/stab976> arXiv:2104.01051 [astro-ph.GA]

[49] Eftekhari, E., La Barbera, F., Vazdekis, A., Allende Prieto, C., Knowles, A.T.: Strong CO absorption features in massive ETGs. *MNRAS* **512**(1), 378–400 (2022) <https://doi.org/10.1093/mnras/stac471> arXiv:2202.08651 [astro-ph.GA]

[50] van Dokkum, P., Conroy, C.: Reconciling M/L Ratios Across Cosmic Time: a Concordance IMF for Massive Galaxies. *ApJL* **973**(1), 32 (2024) <https://doi.org/10.3847/2041-8213/ad77b8> arXiv:2407.06281 [astro-ph.GA]

[51] Ferruit, P., Jakobsen, P., Giardino, G., Rawle, T., Alves de Oliveira, C., Arribas, S., Beck, T.L., Birkmann, S., Böker, T., Bunker, A.J., Charlot, S., de Marchi, G., Franx, M., Henry, A., Karakla, D., Kassin, S.A., Kumari, N., López-Caniego, M., Lützgendorf, N., Maiolino, R., Manjavacas, E., Marston, A., Moseley, S.H., Muzerolle, J., Pirzkal, N., Rauscher, B., Rix, H.-W., Sabbi, E., Sirianni, M., te Plate, M., Valenti, J., Willott, C.J., Zeidler, P.: The Near-Infrared Spectrograph (NIRSpec) on the James Webb Space Telescope. II. Multi-object spectroscopy (MOS). *AA* **661**, 81 (2022) <https://doi.org/10.1051/0004-6361/202142673> arXiv:2202.03306 [astro-ph.IM]

[52] Muzzin, A., Marchesini, D., Stefanon, M., Franx, M., McCracken, H.J., Milvang-Jensen, B., Dunlop, J.S., Fynbo, J.P.U., Brammer, G., Labb  , I., van Dokkum, P.G.: The Evolution of the Stellar Mass Functions of Star-forming and Quiescent Galaxies to $z = 4$ from the COSMOS/UltraVISTA Survey. *ApJ* **777**(1), 18 (2013) <https://doi.org/10.1088/0004-637X/777/1/18> arXiv:1303.4409 [astro-ph.CO]

[53] McCracken, H.J., Milvang-Jensen, B., Dunlop, J., Franx, M., Fynbo, J.P.U., Le F  vre, O., Holt, J., Caputi, K.I., Goranova, Y., Buitrago, F., Emerson, J.P., Freudling, W., Hudelot, P., L  pez-Sanjuan, C., Magnard, F., Mellier, Y., M  ller, P., Nilsson, K.K., Sutherland, W., Tasca, L., Zabl, J.: UltraVISTA: a new ultra-deep near-infrared survey in COSMOS. *AA* **544**, 156 (2012) <https://doi.org/10.1051/0004-6361/201219507> arXiv:1204.6586 [astro-ph.CO]

[54] Muzzin, A., Marchesini, D., Stefanon, M., Franx, M., Milvang-Jensen, B., Dunlop, J.S., Fynbo, J.P.U., Brammer, G., Labb  , I., van Dokkum, P.: A Public K_s - selected Catalog in the COSMOS/ULTRAVISTA Field: Photometry, Photometric Redshifts, and Stellar Population Parameters. *ApJS* **206**(1), 8 (2013) <https://doi.org/10.1088/0067-0049/206/1/8> arXiv:1303.4410 [astro-ph.CO]

[55] Wing, R.F., Ford, W.K. Jr.: The Infrared Spectrum of the Cool Dwarf Wolf 359. *PASP* **81**(482), 527–529 (1969) <https://doi.org/10.1086/128814>

[56] de Graaff, A., Rix, H.-W., Carniani, S., Suess, K.A., Charlot, S., Curtis-Lake, E., Arribas, S., Baker, W.M., Boyett, K., Bunker, A.J., Cameron, A.J., Chevallard, J., Curti, M., Eisenstein, D.J., Franx, M., Hainline, K., Hausen, R., Ji, Z., Johnson, B.D., Jones, G.C., Maiolino, R., Maseda, M.V., Nelson, E., Parlanti, E., Rawle, T., Robertson, B., Tacchella, S.,   bler, H., Williams, C.C., Willmer, C.N.A., Willott, C.: Ionised gas kinematics and dynamical masses of $z \gtrsim 6$ galaxies from JADES/NIRSpec high-resolution spectroscopy. *AA* **684**, 87 (2024) <https://doi.org/10.1051/0004-6361/202347755> arXiv:2308.09742 [astro-ph.GA]

[57] Slob, M., Kriek, M., Beverage, A.G., Suess, K.A., Barro, G., Bezanson, R., Brammer, G., Cheng, C.M., Conroy, C., de Graaff, A., F  rster Schreiber, N.M., Franx, M., Lorenz, B., Mancera Pi  a, P.E., Marchesini, D., Muzzin, A., Newman, A.B., Price, S.H., Shapley, A.E., Stefanon, M., van Dokkum, P., Weisz, D.R.: The JWST-SUSPENSE Ultradeep Spectroscopic Program: Survey Overview and Star Formation Histories of Quiescent Galaxies at $1 < z < 3$. *ApJ* **973**(2), 131 (2024) <https://doi.org/10.3847/1538-4357/ad65ff> arXiv:2404.12432 [astro-ph.GA]

[58] Scoville, N., Aussel, H., Benson, A., Blain, A., Calzetti, D., Capak, P., Ellis, R.S., El-Zant, A., Finoguenov, A., Giavalisco, M., Guzzo, L., Hasinger, G., Koda, J., Le F  vre, O., Massey, R., McCracken, H.J., Mobasher, B., Renzini, A., Rhodes, J., Salvato, M., Sanders, D.B., Sasaki, S.S., Schinnerer, E., Sheth, K., Shopbell, P.L., Taniguchi, Y., Taylor, J.E., Thompson, D.J.: Large Structures and Galaxy Evolution in COSMOS at $z < 1.1$. *ApJS* **172**(1), 150–181 (2007) <https://doi.org/10.1086/516751> arXiv:astro-ph/0612384 [astro-ph]

[59] Bushouse, H., Eisenhamer, J., Dencheva, N., Davies, J., Greenfield, P., Morrison, J., Hodge, P., Simon, B., Grumm, D., Droettboom, M., Slavich, E., Sosey, M., Pauly, T., Miller, T., Jedrzejewski, R., Hack, W., Davis, D., Crawford, S., Law, D., Gordon, K., Regan, M., Cara, M., MacDonald, K., Bradley, L., Shanahan, C., Jamieson, W., Teodoro, M., Williams, T., Pena-Guerrero, M.: JWST Calibration Pipeline. <https://doi.org/10.5281/zenodo.10022973> . <https://doi.org/10.5281/zenodo.10022973>

[60] Moffat, A.F.J.: A Theoretical Investigation of Focal Stellar Images in the Photographic Emulsion and Application to Photographic Photometry. *AA* **3**, 455 (1969)

[61] Shuntov, M., Akins, H.B., Paquereau, L., Casey, C.M., Ilbert, O., Arango-Toro, R.C., McCracken, H.J., Franco, M., Harish, S., Kartaltepe, J.S., Koekemoer, A.M., Yang, L., Huertas-Company, M., Berman, E.M., McCleary, J.E., Toft, S., Gavazzi, R., Achenbach, M.J., Bertin, E., Brinch, M., Champagne, J., Chartab, N., Drakos, N.E., Egami, E., Endsley, R., Faisst, A.L., Fan, X., Flayhart, C., Hartley, W.G., Hatamnia, H., Gozaliasl, G., Gentile, F., Jermann, I., Jin, S., Kakiuchi, K., Khostovan, A.A., Kümmel, M., Laigle, C., Laishram, R., Lambrides, E., Liu, D., Lyu, J., Magdis, G., Mobasher, B., Moutard, T., Renzini, A., Robertson, B.E., Schefer, M., Scognamiglio, D., Scoville, N., Sattari, Z., Sanders, D.B., Taamoli, S., Trakhtenbrot, B., Valentino, F., Wang, F., Weaver, J.R., Yang, J.: COSMOS2025: The COSMOS-Web galaxy catalog of photometry, morphology, redshifts, and physical parameters from JWST, HST, and ground-based imaging. arXiv e-prints, 2506–03243 (2025) <https://doi.org/10.48550/arXiv.2506.03243> arXiv:2506.03243 [astro-ph.GA]

[62] Peng, C.Y., Ho, L.C., Impey, C.D., Rix, H.-W.: Detailed Decomposition of Galaxy Images. II. Beyond Axisymmetric Models. *ApJ* **139**(6), 2097–2129 (2010) <https://doi.org/10.1088/0004-6256/139/6/2097> arXiv:0912.0731 [astro-ph.CO]

[63] Choi, J., Dotter, A., Conroy, C., Cantiello, M., Paxton, B., Johnson, B.D.: Mesa Isochrones and Stellar Tracks (MIST). I. Solar-scaled Models. *ApJ* **823**(2), 102 (2016) <https://doi.org/10.3847/0004-637X/823/2/102> arXiv:1604.08592 [astro-ph.SR]

[64] Villaume, A., Conroy, C., Johnson, B., Rayner, J., Mann, A.W., van Dokkum, P.: The Extended IRTF Spectral Library: Expanded Coverage in Metallicity, Temperature, and Surface Gravity. *ApJS* **230**(2), 23 (2017) <https://doi.org/10.3847/1538-4365/aa72ed> arXiv:1705.08906 [astro-ph.SR]

[65] Sánchez-Blázquez, P., Peletier, R.F., Jiménez-Vicente, J., Cardiel, N., Cenarro, A.J., Falcón-Barroso, J., Gorgas, J., Selam, S., Vazdekis, A.: Medium-resolution Isaac Newton Telescope library of empirical spectra. *MNRAS* **371**(2), 703–718 (2006) <https://doi.org/10.1111/j.1365-2966.2006.10699.x> arXiv:astro-ph/0607009 [astro-ph]

[66] Mann, A.W., Feiden, G.A., Gaidos, E., Boyajian, T., von Braun, K.: How to Constrain Your M Dwarf: Measuring Effective Temperature, Bolometric Luminosity, Mass, and Radius. *ApJ* **804**(1), 64 (2015) <https://doi.org/10.1088/0004-637X/804/1/64> [arXiv:1501.01635](https://arxiv.org/abs/1501.01635) [astro-ph.SR]

[67] Salpeter, E.E.: The Luminosity Function and Stellar Evolution. *ApJ* **121**, 161 (1955) <https://doi.org/10.1086/145971>

[68] Foreman-Mackey, D., Hogg, D.W., Lang, D., Goodman, J.: emcee: The MCMC Hammer. *PASP* **125**(925), 306 (2013) <https://doi.org/10.1086/670067> [arXiv:1202.3665](https://arxiv.org/abs/1202.3665) [astro-ph.IM]

[69] Renzini, A., Ciotti, L.: Transverse Dissections of the Fundamental Planes of Elliptical Galaxies and Clusters of Galaxies. *ApJL* **416**, 49 (1993) <https://doi.org/10.1086/187068>

[70] Cheng, C.M., Kriek, M., Beverage, A.G., Slob, M., Bezanson, R., Franx, M., Leja, J., Mancera Piña, P.E., Suess, K.A., van der Wel, A., van de Sande, J., van Dokkum, P.G.: Ages and metallicities of quiescent galaxies: confronting broadband (UVJ) colours with stellar absorption lines. *MNRAS* **540**(2), 1527–1543 (2025) <https://doi.org/10.1093/mnras/staf806> [arXiv:2505.08858](https://arxiv.org/abs/2505.08858) [astro-ph.GA]

[71] Cheng, C.M., Slob, M., Kriek, M., Beverage, A.G., Barro, G., Bezanson, R., de Graaff, A., Förster Schreiber, N.M., Lorenz, B., Marchesini, D., Martín-Navarro, I., Muzzin, A., Newman, A.B., Price, S.H., Suess, K.A., van der Wel, A., van de Sande, J., van Dokkum, P.G., Weisz, D.R.: Building up JWST-SUSPENSE: inside-out quenching at cosmic noon from age, Fe-, and Mg-abundance gradients. *arXiv e-prints*, 2509–12316 (2025) <https://doi.org/10.48550/arXiv.2509.12316> [arXiv:2509.12316](https://arxiv.org/abs/2509.12316) [astro-ph.GA]

[72] Jafariyazani, M., Newman, A.B., Mobasher, B., Belli, S., Ellis, R.S., Patel, S.G.: Resolved Multi-element Stellar Chemical Abundances in the Brightest Quiescent Galaxy at $z \sim 2$. *ApJL* **897**(2), 42 (2020) <https://doi.org/10.3847/2041-8213/aba11c> [arXiv:2007.00205](https://arxiv.org/abs/2007.00205) [astro-ph.GA]

[73] Bezanson, R., van der Wel, A., Pacifici, C., Noeske, K., Barišić, I., Bell, E.F., Brammer, G.B., Calhau, J., Chauke, P., van Dokkum, P., Franx, M., Gallazzi, A., van Houtd, J., Labbé, I., Maseda, M.V., Muños-Mateos, J.C., Muzzin, A., van de Sande, J., Sobral, D., Straatman, C., Wu, P.-F.: Spatially Resolved Stellar Kinematics from LEGA-C: Increased Rotational Support in $z \sim 0.8$ Quiescent Galaxies. *ApJ* **858**(1), 60 (2018) <https://doi.org/10.3847/1538-4357/aabc55> [arXiv:1804.02402](https://arxiv.org/abs/1804.02402) [astro-ph.GA]

[74] Cappellari, M.: Full spectrum fitting with photometry in PPXF: stellar population versus dynamical masses, non-parametric star formation history and metallicity for 3200 LEGA-C galaxies at redshift $z \approx 0.8$. *MNRAS* **526**, 3273–3300 (2023) <https://doi.org/10.1093/mnras/stad2597> [2208.14974](https://arxiv.org/abs/2208.14974)

[75] Bertin, E., Arnouts, S.: SExtractor: Software for source extraction. *AAS* **117**, 393–404 (1996) <https://doi.org/10.1051/aas:1996164>

Methods

Observing Strategy and Data Reduction

In order to robustly constrain the IMF, we require extremely deep spectra covering optical and near-infrared wavelengths. To achieve this beyond the local Universe, we take advantage of the optical spectra from the third data release of the Large Early Galaxy Astrophysics Census (LEGA-C), a European Southern Observatory (ESO) Public Spectroscopic survey of 3600 galaxies at $0.6 \lesssim z \lesssim 1.0$. These deep (20 hr integration), $R \sim 3500$ spectra were collected over 128 nights using the VIMOS spectrograph on the ESO Very Large Telescope (VLT), resulting in an average $S/N \sim 20 \text{ \AA}^{-1}$ (see [8] for details).

At $z \sim 0.7$, the LEGA-C observing strategy results in a rest-frame wavelength range of $\sim 3660 - 5120 \text{ \AA}$, capturing several Balmer features and metal lines that are sensitive to age, $[\text{Fe}/\text{H}]$, and several elemental abundances. However, features that are sensitive to the ratio of dwarf to giant stars, which can be used to constrain the IMF [12], are located in the rest-frame near-infrared. To capture these features, we extend the LEGA-C spectra with extremely deep Near Infrared Spectrograph micro shutter array (NIRSpec/MSA, [51]) spectra from the *JWST*-IMFERNO program (Initial Mass Function of Early Red NIRSpec Objects, ID 5629, PIs: Kriek, Beverage, and Cheng), executed on May 3-4 and 25, 2025.

To select our targets for *JWST*-IMFERNO, we identified quiescent targets with the *UVJ* classification from [52], using the UltraVISTA [53] DR3 K_s -band catalogue [54]. In order to achieve our S/N requirements, we required an H -band magnitude < 21.5 . We additionally required the NIRSpec/MSA spectra to capture IMF sensitive features including NaI ($\sim 8180 - 8200 \text{ \AA}$), CaT ($\sim 8475 - 8725 \text{ \AA}$), and the Wing-Ford band where possible ($\sim 9905 - 9945 \text{ \AA}$, [55]). This was feasible for galaxies at $z \sim 0.7$ using the G140M-F100LP disperser-filter combination, allowing us to obtain spectra covering $9700 - 18400 \text{ \AA}$, with a spectral resolution of $R \sim 1300$ [e.g. 56, 57]. This wavelength range corresponds to a rest-frame wavelength coverage of $\sim 5660 - 10780 \text{ \AA}$. We identified one extraordinary pointing for which we observed 13 massive ($10.28 \lesssim \log(M_*/M_\odot) \lesssim 11.59$, assuming a Kroupa IMF [8, 16]), quiescent galaxies at $z \sim 0.7$ which have LEGA-C optical spectra and COSMOS-Web imaging [9]. Nine of the 13 galaxies have sufficient S/N to simultaneously constrain ages, elemental abundances, and IMF variations. We note that all of our targets fit in one pointing due to the “COSMOS Wall” structure at $z \sim 0.73$ [58]. Thus, our targets are also located in an old region of the $z \sim 0.7$ Universe, reinforcing the connection between our targets and massive galaxies in the early Universe.

The galaxies were observed using a custom two-point nod pattern with a two-micro-shutter ($1''.06$) offset in the cross-dispersion direction, following the *JWST*-SUSPENSE program [57]. With this nodding pattern and large offset, we mitigate the self-subtraction of continuum emission for our extended targets in the data reduction process. To correct for detector and micro shutter artifacts we observed our galaxies in two nearly identical, MSA configurations, offset by 3 micro shutters in the dispersion direction. Our nod-dither pattern resulted in four observing positions. While it was not possible to observe all filler targets in all four positions, seven of our nine primary

targets presented in this work were covered by all positions resulting in a total on-source integration time of 31.2 hrs. Two primary targets (1155117 and 1158527) were only fully observed in three nod-dither positions due to slit failures during one visit. However, these two targets still have high enough S/N to be included in our final sample. To ensure sufficient empty sky for background calibration, we observed the primary targets with slitlets consisting of five to nine shutters.

We reduce the data to 2D flux calibrated spectra using the JWST Science Calibration Pipeline [59] v1.17.1 and version 1322 of the Calibration Reference Data System (CRDS). We add a $1/f$ correlated vertical readout noise correction to this pipeline, as described in [57]. After generating the 2D spectra via the pipeline, we use an optimal extraction algorithm with a Moffat profile [60] to extract the 1D spectra. Since the two dithers in our observations have slightly different MSA configurations, we reduce the dithers separately and combine the resulting 1D spectra. Finally, to ensure the LEGA-C and IMFERNO spectra are on the same flux scale, we re-scale the 1D spectra from each survey to the overlapping COSMOS2025 [61] photometry. For each galaxy in our sample, we derive morphological parameters by fitting COSMOS-Web F150W photometry [9] with GALFIT [62].

Full-spectrum fitting

To measure ages, elemental abundances, and low-mass IMF slopes, we fit the combined LEGA-C and IMFERNO spectra of 9 massive, quiescent galaxies at $z \sim 0.7$ with the ABSORPTION LINE FITTER (ALF), a full spectrum stellar population synthesis (SPS) model [12, 15]. The ALF models are built on empirical simple stellar populations (SSPs), created using the MIST isochrones [63] and the Spectral Polynomial Interpolator (SPI, [64]). We use the MILES empirical spectral library [65], the E-IRTF stellar library [64], and a large sample of M-dwarf spectra [66] with SPI. We additionally use a theoretical stellar library (C3K, see [12]) to ensure the quality of interpolation at the boundaries of the empirical parameter space. The ALF models allow for variable abundance patterns by differentially including theoretical element response functions. We explore an empirical parameter space spanning $-2.0 \lesssim [\text{Fe}/\text{H}] \lesssim 0.5$ and $3.5 \lesssim \log(T_{\text{eff}}/\text{K}) \lesssim 3.9$, which is set by the combined E-IRTF and [66] samples. With these components, ALF develops stellar spectra as a function of T_{eff} , surface gravity, and metallicity from a data-driven model.

We parameterize the IMF as a double broken power-law with break points at $m = 0.5 \text{ M}_{\odot}$ and 1 M_{\odot} , similar to the Kroupa IMF [16], and a fixed low-mass cutoff (m_c) at 0.08 M_{\odot} . Above 1.0 M_{\odot} , the IMF slope is assumed to have the Salpeter [67] value of 2.35:

$$\frac{dN}{dm} = \begin{cases} k_1 m^{-\alpha_1}, & 0.08 < m < 0.5 \\ k_2 m^{-\alpha_2}, & 0.5 < m < 1.0 \\ k_3 m^{-2.35}, & m \geq 1.0 \end{cases} \quad (1)$$

For a MW IMF, we use the Kroupa [16] values of $\alpha_1 = 1.3$ and $\alpha_2 = 2.3$. This IMF parameterization is shown in Extended Data Figure 4, for a Kroupa IMF, a Salpeter IMF, and the best-fit IMFs of the IMFERNO sample.

To derive stellar population parameters, ALF fits a high-order Chebyshev polynomial to the ratio of the data to the model, to continuum-normalize the target

spectrum. Using a FORTRAN implementation of the Markov chain Monte Carlo algorithm (MCMC), `emcee` [68], ALF samples the posteriors of 46 different stellar parameters, allowing for arbitrary variation in stellar age, elemental abundances, and the two low-mass slopes of the IMF (see Equation 1). It also fits for systematic parameters to characterize observed errors, including a jitter term. Additionally, it calculates M/L ratios by computing the mass in stars and remnants (using the prescription in [69]), assuming an IMF, and dividing this by the integral of the spectrum over the filter of interest (*HST*/ACS-F814W in our case). M/L ratios are calculated assuming the best-fit free IMF and Kroupa IMF for each fit. For details, see [12] and [15].

We smooth the ALF models to the instrumental resolution of the LEGA-C and NIRSpec/MSA observations before fitting. Since the instrumental resolution of the NIRSpec/MSA depends strongly on the source morphology and position in the slit [56, 57], we derive the instrumental resolution for each individual galaxy using MSAFIT [56] and COSMOS-Web F150W NIRCam imaging [9], following [57]. The derived instrumental resolution for each galaxy differs from pre-launch estimates¹ for the G140M disperser, by a wavelength independent factor. We thus use the pre-launch estimated resolution curve, multiplied by the derived offset, as the final instrumental resolution for each galaxy.

Following the methodology of [11, 70], we fit each spectrum using 1024 walkers, 20000 burn-in steps, and a 1000 step production run. We examine 500 MCMC chains per fit. We fit a single age, and avoid the walkers getting trapped at an unrealistically high age by initializing the age of each galaxy with a random value drawn from a uniform distribution centred at 3 Gyr. Additionally, we set the upper limit of the age prior to be the age of the Universe at the redshift of each galaxy, plus 2 Gyr to allow for uncertainties. We note that ALF can fit spectra between 3700 – 24000 Å and can be used for stellar populations that are older than 1 Gyr.

Our fiducial results consist of fits to the full spectra, fitting the LEGA-C and IMFERNO spectra simultaneously (although note that we additionally fit the LEGA-C and IMFERNO spectra separately for testing purposes, see the next Section). We mask strong emission lines, including [OIII], [SII], and the H α +[NII] complex, when they are present. Where possible, we fit the wavelength ranges 3700 – 4700 Å, 4700 – 5200 Å, 5600 – 6000 Å, 6000 – 6700 Å, 8000 – 8920 Å, 8920 – 9630 Å, 9630 – 10150 Å, and 10150 – 10800 Å, excluding the regions between 7000 – 8000 Å due to broad TiO absorption (this is in line with previous work, see, e.g. [13, 17, 47]). We also fit the spectra including the region between 7000 – 8000 Å and find that while the results are relatively consistent with our fiducial fit, including this TiO absorption introduces extremely large errorbars for some of our α_{IMF} parameters. In our fiducial fit, we include the NaD absorption feature near ~ 5900 Å, which is crucial for constraining the upper limit of the IMF-degenerate Na-abundance [12]. However, since NaD can be affected by the interstellar medium [12], we also test masking this feature. Similar to our TiO test, we find that while the results are consistent, some of the errorbars on α_{IMF} are inflated. Finally, we note that for some of the IMFERNO spectra, the IMF-sensitive Wing-Ford band [55] falls in the detector gap (see Figure 1). Nonetheless,

¹<https://jwst-docs.stsci.edu/jwst-near-infrared-spectrograph/nirspec-instrumentation/nirspec-dispersers-and-filters>

it has been shown that while all three features (NaI, CaT, and the Wing-Ford band) are important for robustly constraining the IMF, the exact shape of the IMF and trends with bottom-heaviness are not sensitive to any one feature. In other words, the results remain consistent when excluding individual features, as IMF variations affect the entire spectrum (see [13, 17]). We show our final fits to the LEGA-C spectra in Extended Data Figure 6 and our final fits to the IMFERNO spectra in Figure 1, but again note that we fit the two sides of each spectrum simultaneously.

Finally, for each galaxy we calculate α_{IMF} (the ratio between the M/L where we allow the IMF to vary and the M/L where we fix a MW IMF) and use this α_{IMF} value to correct the stellar mass. These masses were originally constrained by fitting the photometric spectral energy distributions (from the UltraVISTA K_s -band catalogue [54]) of the galaxies with the MAGPHYS code [28]. They have been scaled to the total stellar mass using the total luminosity of the best-fit Sérsic profile (see [29]). We correct the MAGPHYS masses with our best-fit α_{IMF} values instead of extracting masses from our ALF fits as MAGPHYS considers star-formation histories and dust more rigorously than ALF (which only has two simple star-formation history options and does not account for dust).

Stellar velocity dispersions and virial masses

The optical LEGA-C and near-infrared IMFERNO data were obtained with two different instruments. Thus, we must consider the fact that we are not examining exactly the same spatial areas of each galaxy in the optical and near-infrared, due to differences in apertures, point-spread functions, slit orientations, and slit offsets with respect to galaxy centres. In particular, our measurements may be affected by stellar population gradients [11, 71, 72] and galaxy dynamics [34, 73]. Stellar population gradients in LEGA-C galaxies have been found to be relatively weak [11]. In contrast, the velocity dispersions may be affected by differences in slit orientation, as the LEGA-C slits are oriented in the north-south direction and the IMFERNO slitlets have a position angle of ~ 247 degrees. This is especially the case if the galaxies are rotating [73].

To assess – and, if needed, correct for – velocity dispersion differences, we fit the IMFERNO spectra in isolation (i.e. without combining them with the optical LEGA-C spectra), and compare the recovered velocity dispersions ($\sigma_v, \text{IMFERNO}$) to those from the LEGA-C survey, measured with PPXF ([74], $\sigma_v, \text{LEGA-C}$) [8, 38]. For galaxies whose σ_v 's are offset by more than 1σ , we derive and apply a correction factor by subtracting the two σ_v 's in quadrature. In this way, we effectively broaden the spectrum with the lowest velocity dispersion to the same σ_v . In total, we correct 4/9 galaxies for velocity dispersion offsets. We re-fit the corrected full spectra (i.e. LEGA-C + IMFERNO, shown in the body of the paper) and the individual sides of the spectra to assess the effect of our correction. We show this effect in Extended Data Figure 7. We note that this correction does not affect our conclusions. In particular, the α_{IMF} parameters for individual galaxies are consistent between the fits to the uncorrected and corrected spectra (see the right panel of Extended Data Figure 7).

For the three galaxies for which $\sigma_v, \text{IMFERNO}$ is greater than $\sigma_v, \text{LEGA-C}$ (likely due to different slit alignments along the kinematic major axes), we also correct their virial masses. In particular, we multiply the virial masses from [23] by a factor of

$\sigma_{v, \text{IMFERNO}}^2 / \sigma_{v, \text{LEGA-C}}^2$. These corrected virial masses are shown throughout the paper. We additionally use the maximum velocity dispersion between LEGA-C and IMFERNO as the fiducial σ_v throughout the paper, as this is more representative of the galaxy's velocity dispersion. This is due to the fact that the lower σ_v may neglect part of the kinematics if the slit is oriented along the minor axis.

Table 1 Sample properties.

ID	RA ¹ (hh:mm:ss)	Dec ¹ (dd:mm:s)	z_{spec}^2	H^3 (mag)
1155117	09:59:40.85	+02:30:51.2	0.6984	20.5
1158527	09:59:38.92	+02:30:59.7	0.7281	19.9
1166579	09:59:39.77	+02:31:16.7	0.7286	18.6
1163505	09:59:30.41	+02:31:07.4	0.7303	19.8
1146989	09:59:33.55	+02:30:20.2	0.7324	20.2
1176261	09:59:39.27	+02:32:04.2	0.7327	20.8
1134272	09:59:46.85	+02:29:08.4	0.7340	18.4
1130066	09:59:36.93	+02:29:20.3	0.7347	21.2
1156232	09:59:32.99	+02:30:47.2	0.7357	19.2

¹Derived from running SOURCEEXTRACTOR [75] on the COSMOS-Web F150W images [9].

²From the LEGA-C survey [8].

³From the UltraVISTA K-band photometric catalogue [54].

Extended Data.

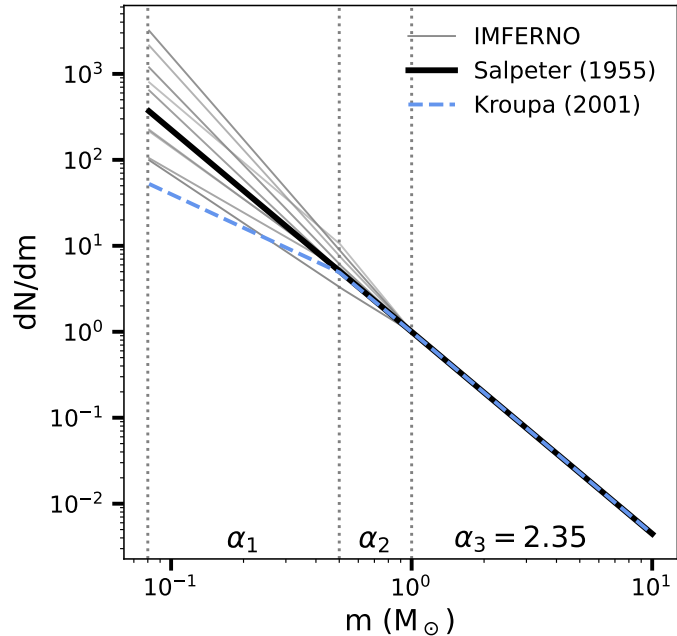


Fig. 4 IMF shapes for the IMFERNO sample (grey lines), compared to Kroupa (dashed blue line, [16]) and Salpeter (black line, [67]) IMFs. The double broken power law IMF is parameterized as in Equation 1 and shown on the y -axis for a range of stellar masses (x -axis). We indicate the breakpoints of the IMF with vertical dotted grey lines.

Table 2 Results from our ALF fits to the combined LEGA-C and *JWST*-IMFERNNO spectra. σ_v represents the largest σ_v between the LEGA-C reported value and the value that we obtain from fitting the IMFERNNO spectra in isolation. M/L ratios are derived in the *HST*/ACS-F814W band.

ID	$\log(M_{\text{vir}})$ (M_{\odot})	$\log(M_*)$ (free, M_{\odot})	$\log(M_*)^1$ (MW, M_{\odot})	σ_v (km/s)	Age (Gyr)	[Fe/H]	M/L (free)	M/L (MW)	α_{IMF}
1155117	10.50 ± 0.06	$10.30^{+0.25}_{-0.12}$	10.28	170 ± 8^1	$1.31^{+0.07}_{-0.06}$	$0.03^{+0.06}_{-0.03}$	$6.95^{+4.14}_{-1.92}$	$6.53^{0.13}_{0.12}$	$1.05^{+0.60}_{-0.29}$
1158527	10.79 ± 0.06	$11.43^{+0.09}_{-0.10}$	10.70	133 ± 6	$2.83^{+0.07}_{-0.08}$	$0.14^{+0.03}_{-0.02}$	$59.57^{+12.10}_{-13.05}$	$11.09^{0.17}_{0.16}$	$5.36^{+1.15}_{-1.17}$
1166579	11.92 ± 0.07	$11.94^{+0.09}_{-0.09}$	11.46	279^{+9}_{-8}	$7.54^{+0.84}_{-1.12}$	$0.06^{+0.05}_{-0.05}$	$66.85^{+13.47}_{+12.47}$	$22.75^{1.23}_{1.21}$	$3.00^{+0.61}_{+0.61}$
1163505	11.03 ± 0.07	$11.11^{+0.42}_{-0.42}$	10.80	195 ± 8^1	$1.90^{+0.06}_{-0.06}$	$-0.01^{+0.04}_{-0.04}$	$16.42^{+15.40}_{-15.40}$	$8.10^{0.14}_{-0.14}$	$2.05^{+1.92}_{-1.92}$
1146989	10.66 ± 0.06	$10.73^{+0.22}_{-0.22}$	10.62	167 ± 5^1	$2.28^{+0.07}_{-0.07}$	$-0.00^{+0.04}_{-0.04}$	$12.53^{+5.97}_{-4.28}$	$9.52^{0.16}_{0.15}$	$1.30^{+0.65}_{-0.65}$
1176261	10.92 ± 0.08	$10.50^{+0.15}_{-0.18}$	10.32	236 ± 16^1	$5.32^{+1.15}_{-1.25}$	$-0.17^{+0.07}_{-0.07}$	$23.33^{+11.87}_{-8.83}$	$15.14^{1.90}_{1.69}$	$1.53^{+0.78}_{-0.78}$
1134272	12.18 ± 0.06	$12.20^{+0.08}_{-0.08}$	11.59	293 ± 8^1	$6.10^{+0.53}_{-0.48}$	$-0.05^{+0.03}_{-0.03}$	$68.94^{+11.35}_{-11.93}$	$16.79^{0.83}_{0.76}$	$4.08^{+0.74}_{-0.74}$
1130066	10.35 ± 0.09	$10.55^{+0.27}_{-0.27}$	10.38	117 ± 6	$3.10^{+0.27}_{-0.27}$	$-0.08^{+0.03}_{-0.03}$	$17.15^{+11.93}_{-11.93}$	$11.59^{0.55}_{0.38}$	$1.47^{+0.93}_{-0.77}$
1156232	11.50 ± 0.06	$11.47^{+0.09}_{-0.09}$	11.01	297 ± 8^1	$4.08^{+0.30}_{-0.28}$	$0.08^{+0.03}_{-0.03}$	$39.70^{+8.30}_{-9.06}$	$13.72^{0.46}_{0.41}$	$2.90^{+0.59}_{-0.64}$

¹From the LEGA-C survey [8].

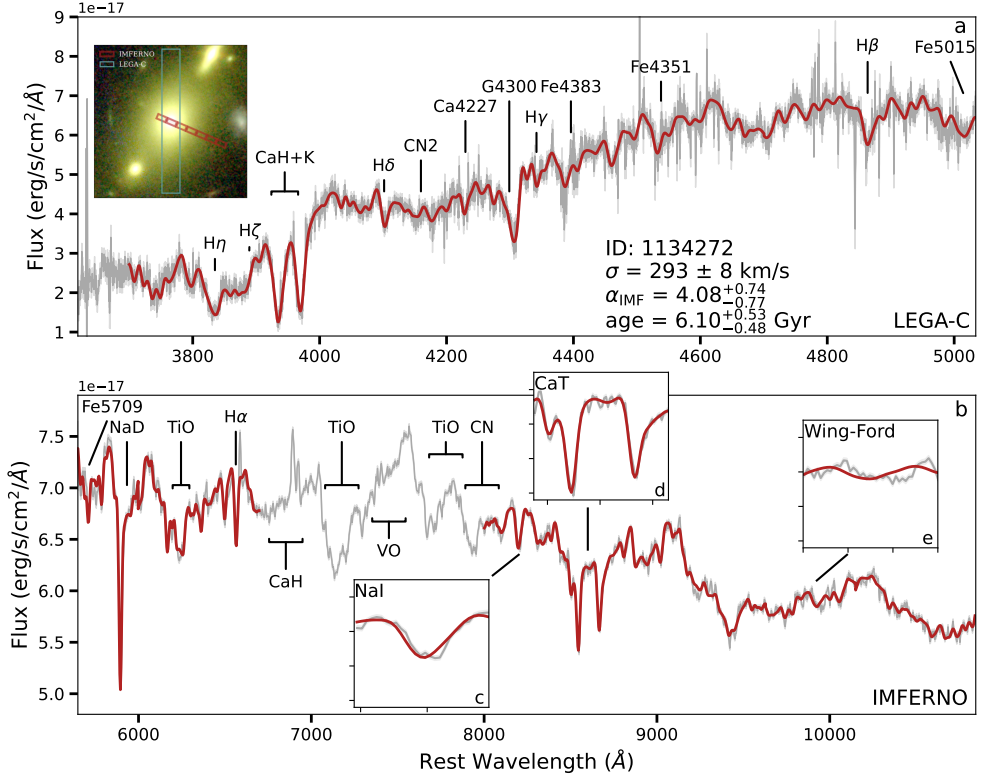


Fig. 5 Example ALF fit to a bottom-heavy galaxy in our sample. The data are shown in grey with shaded regions indicating 1σ uncertainties on the flux, and the best-fit model is shown in red. We show the spectrum from LEGA-C in panel a and the IMFFERNO spectrum in panel b, but we note that we fit the entire wavelength range simultaneously. In the inset panels (panels c-e), we zoom in on three strong absorption features which are sensitive to IMF variations. We continuum-normalize the features in the inset panels, but include the continuum in the main panels.

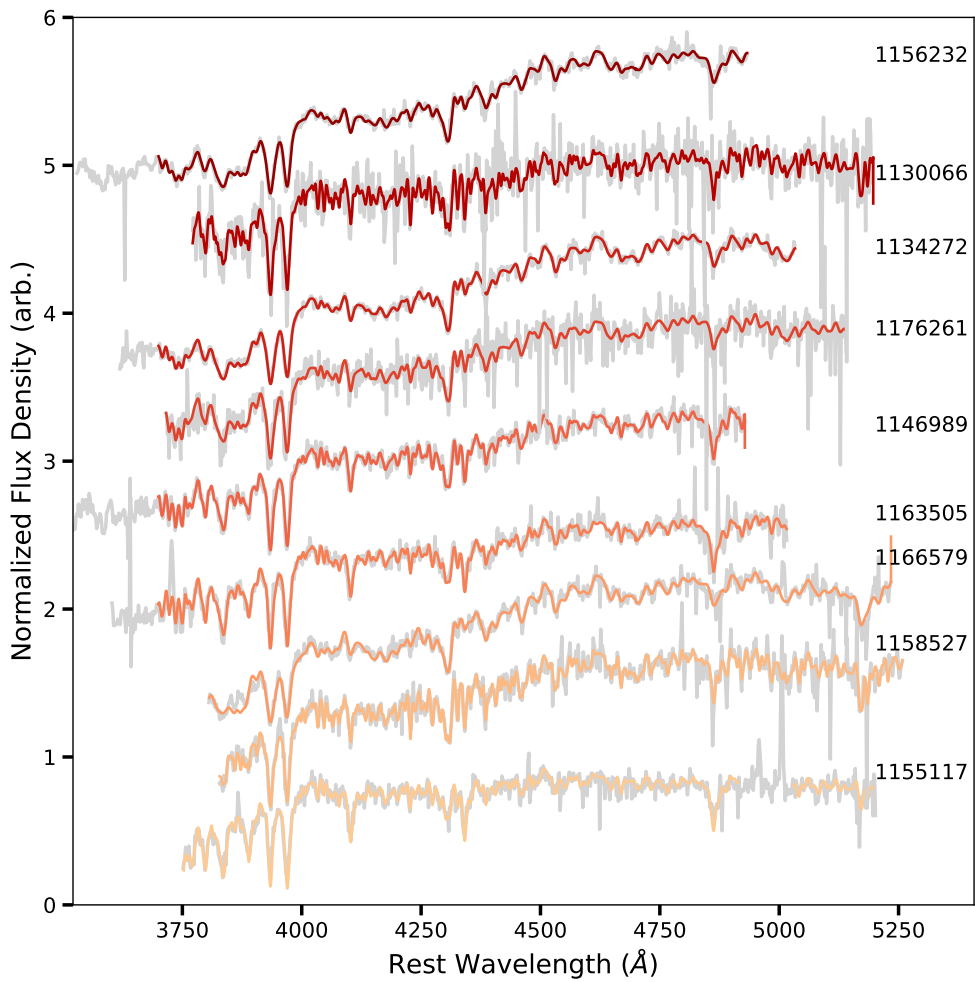


Fig. 6 Similar to Figure 1 but showing the best fits to the bluer sides of the spectra from LEGA-C. Spectra are shown in grey from bottom to top in order of increasing redshift. The best-fitting models are shown as coloured lines, as in Figure 1. We normalize each spectrum and fit by the median value of the flux between $4400 - 4500$ Å. We arbitrarily offset the spectra in the y -direction and median bin the data in bins of 5 pixels for visibility.

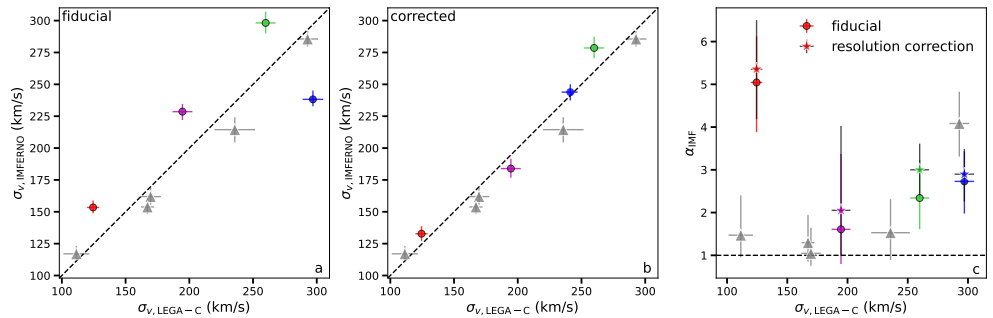


Fig. 7 A demonstration of our velocity dispersion correction to four galaxies in our sample. The colourful points show the galaxies for which we perform the correction and the grey triangles show the galaxies that do not need to be corrected, for comparison. In panel a, we show the fiducial σ_v values from LEGA-C [8, 38] and from fits to the individual IMFERNO spectra. In panel b, we show the corrected σ_v 's. In panel c, we show the effect that the correction has on our derived α_{IMF} .